

Catalysis Science & Technology

Accepted Manuscript



This is an *Accepted Manuscript*, which has been through the Royal Society of Chemistry peer review process and has been accepted for publication.

Accepted Manuscripts are published online shortly after acceptance, before technical editing, formatting and proof reading. Using this free service, authors can make their results available to the community, in citable form, before we publish the edited article. We will replace this *Accepted Manuscript* with the edited and formatted *Advance Article* as soon as it is available.

You can find more information about *Accepted Manuscripts* in the [Information for Authors](#).

Please note that technical editing may introduce minor changes to the text and/or graphics, which may alter content. The journal's standard [Terms & Conditions](#) and the [Ethical guidelines](#) still apply. In no event shall the Royal Society of Chemistry be held responsible for any errors or omissions in this *Accepted Manuscript* or any consequences arising from the use of any information it contains.

ARTICLE

Manipulating the reaction path of the CO₂ hydrogenation reaction in molecular sieves

Cite this: DOI: 10.1039/x0xx00000x

A Borgschulte,^a E. Callini,^b N. Stadie,^b Y. Arroyo,^c M. D. Rossell,^c R. Erni,^c H. Geerlings^d, A. Züttel^{b,e}, D. Ferri^f

Received

[Accepted](#)

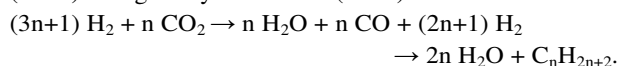
DOI: 10.1039/x0xx00000x

www.rsc.org/

We demonstrate that the kinetics of the Sabatier reaction catalysed by sorption catalysts depends on the nanostructure of the catalyst – sorbent system. The catalysts are prepared by ion exchange of Ni-nitrate solution in two zeolites with different pore size. Beside a different pore size, which enables or hinders the adsorption of the reactants, intermediates and products in the inner of the crystallites, the catalyst systems have slightly different size distribution of the Ni-particles. By studying various catalysts with different Ni-contents we can attribute different catalytic activity and in particular the selectivity to the shape selectivity of the zeolite support. Focus lays on the microstructural characterization of the catalyst. We observe that the selectivity for methane is greatly enhanced if the pore size of the support is larger than 5 Å, while pore sizes of less than 3 Å reduce the overall conversion rate and the selectivity for methane. Thus, Ni on 3A zeolites can be used as low temperature catalysts for the reversed water-gas shift reaction producing carbon monoxide.

A Introduction

Primarily goal of most industrialized chemical processes is the production of a chemical compound at maximum yield. The energy efficiency is important, too, but ranks as a secondary parameter [1]. This is different in chemical processes aiming for the production of a chemical energy carrier. A chemical energy carrier, e.g. hydrogen, is a vector, i.e., it is most important how much energy can be delivered with it considering also the conversion losses; an energy carrier costing more energy for production than it delivers does not make any sense. The energy efficiency of the production and conversion reactions is thus the most relevant parameter. However, in most cases, existing catalysts were developed for technical processes, i.e. highest conversion rate. In this sense, the CO₂ hydrogenation reactions are typical, because relatively good working catalysts are at hand and the corresponding reaction mechanisms are well understood [2] [3]. However, the heat release of the exothermic reactions yielding either methane (n = 1) or higher hydrocarbons (n > 1)



$$\Delta H = -165 \text{ kJ/mol (n = 1)} \rightarrow \Delta H = -115 \text{ kJ/mol (n = 8)} \quad (1)$$

is an energy loss, which cannot be avoided by simply improving kinetics. When producing liquid hydrocarbons, the reaction (1) takes place usually also spatially separated in two reactors, i.e., first producing CO (reversed water-gas shift reaction, RWGS) and then utilizing the Fischer-Tropsch

reactions yielding liquid hydrocarbons [4]. As the RWGS reaction is endothermic, it proceeds at high temperatures only. Therefore, the required heat cannot be taken from the exothermic Fischer-Tropsch reaction, because the corresponding optimal reaction temperature of this reaction is much lower. Thus, production of liquid solar fuels based on the two sub-steps reaction is associated with a significantly greater energy loss than the thermodynamically required one. To reduce the loss, Haije and Geerlings [4] propose the use of sorption catalysis. Here, the exothermic adsorption of water adds up to the overall reaction heat thus reducing the reaction temperature and increasing the conversion efficiency. This is a thermodynamic argumentation: the free energy of the system defines the reaction path. A realization of a sorption reaction should thus not require peculiar “sorption catalysts” – lowering the water partial pressure by plain physical mixture of catalysts and sorbent should be sufficient to shift the equilibrium of the Sabatier reaction towards the product side as has indeed been demonstrated by [5]. However, in this paper, we demonstrate that the kinetics of the reaction and thus eventually the reaction path depends on the nanostructure of the catalyst – sorbent system, i.e. the sorption catalyst. This might be seen as additional effort for the technical realization of sorption catalysts, but can also be exploited. The idea is the following. CO is an intermediate occurring on most metallic catalysts during CO₂ hydrogenation (eq. 1) [6] [3]. Subsequently, the CO is further reduced. We demonstrate that this subsequent step is impeded, if the reaction takes place in composite catalysts with

specific mesoporous structure thereby increasing the selectivity for CO instead of hydrocarbons – making use of the so-called shape-selectivity.

The shape-selectivity of zeolites has wide applications in catalysis – examples are reactant selectivity (e.g. dewaxing), product shape selectivity (e.g. toluene disproportionation), and transition-state selectivity (e.g. alkylation of aromatics), see, e.g., Refs. [7], [8], [9], [10], [11]. The basic idea is that the pore size inside the porous structure interferes with the molecular size of the reactants, products, and transitions states, respectively. The above given examples depict situations in which the corresponding molecules are rather large (long chain hydrocarbons, benzene rings, etc.) and thus their size and shape and their interactions with the pore walls are well defined.

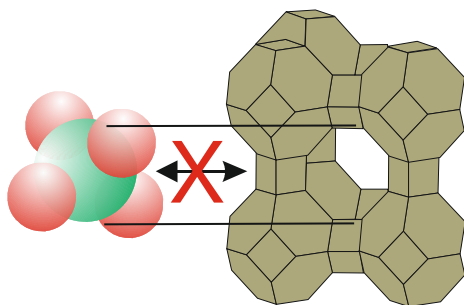


Figure 1: Illustration of the shape-selectivity in molecular sieves. CH₄ (kinetic diameter around 3.8 Å) is adsorbed in zeolite 5A (5 Å pore size), but not in zeolite 3A. The picture is misleading, though: the size of a molecule is not directly related to its atomic structure, but to its ‘kinetic diameter’, which is derived from viscosity or diffusion experiments [12].

, This is not the case for small molecules, which are of interest in energy conversion processes. The Linde type A (LTA) zeolite has pore diameters (window size) close to the kinetic diameters of small molecules (‘molecular sieves’) [13] – in particular, while the pore diameter of zeolite 5A is larger, the one of zeolite 3A is smaller than the kinetic diameter of CH₄. Thus CH₄ cannot easily leave the 3 Å pores (the encapsulation of CH₄ is a very slow process [14]). However, unfortunately, CO₂ and CO have similar diameters and cannot enter such small pores either. The gas kinetic diameter is an empirical parameter, which is usually derived either from the viscosity of the corresponding gas or its (self) diffusion coefficient. [12]. Accordingly the numbers differ slightly. The uptake of the corresponding molecule by the zeolite provides a better and more direct characterization about whether the gas molecules can enter the inner pores. Furthermore, the selectivity of a reaction, in this case of the CO₂ hydrogenation, depends significantly on the particle size of the catalytically active metal [15] [16]. Although we do not want to focus on this effect here, the particle size of the Ni-particles in the zeolite catalyst is altered by the specific zeolite and preparation method. This side effect is carefully investigated; and by a comparison of the adsorptive and structural properties with the measured reactivity and selectivity we are able to demonstrate the shape selectivity of Ni-LTA zeolite systems for CO₂-hydrogenation.

B Materials and methods

Nickel nitrate (Ni(NO₃)₂·6H₂O) (Sigma Aldrich) and molecular sieves (zeolite 3A/5A) with pore sizes of 3 and 5 Å (pellets, 1.6 mm, Sigma Aldrich) with linear formulae K_nNa_{12-n}[(AlO₂)₁₂(SiO₂)₁₂] · xH₂O and Ca_nNa_{12-2n}[(AlO₂)₁₂(SiO₂)₁₂] · xH₂O, respectively, were used in the preparation of nickel sorption catalysts. The alkaline / earth alkaline zeolite was exchanged using Nickel nitrate aqueous solution with different concentrations at room temperature for 24 h (0.1 M/ 5M). Then, the zeolite was washed with deionized water and dried under an air stream at 100°C for two days. Subsequently, the sample was reduced in a hydrogen flow at 650°C for two hours.

The measurements of the catalytic activity were performed using a stainless steel tubular flow reactor with a length of 450 mm and a diameter of 18 mm. Typical catalyst mass was 13 g (total) with a volume of 25 ml. The gas flows were controlled by thermal mass flow meters from MKS Instruments connected to a Labview interface. Typical flow rates were 50 ml/min CO₂, and 400 ml/min H₂ corresponding to a space velocity of 1000 h⁻¹. A ratio of 8:1 for H₂:CO₂ was chosen to not favour the RWGS-reaction thermodynamically and to be more sensitive to kinetic effects. The pressure was 1.2 bar. The exhaust gases were analysed using a Fourier transform infrared (FT-IR) spectrometer (Alpha, Bruker) equipped with an 8 cm gas cell. The exhaust gas was diluted with N₂ to avoid saturation of the infrared spectrum and the condensation of water. The temperature dependence of the conversion at constant reactants’ flows was monitored by cooling down from highest temperature. For transient measurements at isothermal conditions, the catalyst was dried in hydrogen at high temperature. After equilibration to the desired measurement temperature, the CO₂ flow was switched on.

The catalysts were characterized for their specific surface area (BET method) and Ni content, metal area and crystallite size. The BET surface area of the sample was extracted from nitrogen adsorption isotherms at 77 K measured with a BELSORPmax (BEL, Japan). In addition, H₂ and CO₂ adsorption isotherms at room temperature were conducted using the same apparatus. By performing subsequent hydrogen adsorption isotherms, the amount of chemisorbed hydrogen was determined.

For microstructural characterization at the μm-scale, secondary electron SEM imaging was carried out with a FEI ESEM XL30 at an acceleration voltage of 20 kV. The SEM is equipped with an energy-dispersive X-ray spectroscopy (EDX) for elemental analysis. The structure at the nano-scale was examined by scanning transmission electron microscopy (STEM) with a JEOL 2200FS TEM. For the electron tomography, high angle annular dark-field (HAADF)-STEM images were recorded at 2° tilt intervals between -70° to 70°. The images were aligned

using the StackReg plugin for the image processing software ImageJ. The 3D reconstruction was computed using 30 cycles of simultaneous iterative reconstruction technique (SIRT) implemented in TomoJ (ImageJ plugin). The 3D projections were generated with the Amira visualization program.

Diffuse reflectance infrared Fourier transform spectroscopy (DRIFTS) combined with mass spectrometry has been used to probe the surface species (reactants, intermediates and products) during reaction. The DRIFT spectra with a resolution of 4 cm^{-1} were collected using a Vertex 70 spectrometer (Bruker) equipped with a mirror unit (Praying Mantis, Harrick) and a liquid nitrogen cooled MCT detector. The commercial Harrick cell (HVC-DRP-3) was windowed with a flat CaF_2 window rather than the conventional dome and was attached to a gas manifold system. The gas exiting the cell was analysed online using a mass spectrometer (Pfeiffer, Omnistar) (see also Ref. [2]). After in situ reduction in 80 vol% H_2/Ar at 500°C and cooling to 420°C , the sample (80 mg) was exposed to the $\text{H}_2:\text{CO}_2$ 8:1 reaction mixture at a total flow of 54 ml/min.

C Results and discussions

Catalytic Activity

We measured the temperature dependence of the CO_2 reduction under excess of hydrogen rate at a given space velocity for various catalysts made of Ni-impregnated 3A zeolite and 5A zeolite, respectively with different Ni-loading. The measurements as shown in **Figure 2** and **Figure 3** were conducted after long term equilibration thereby eliminating the water sorption function of the zeolite.

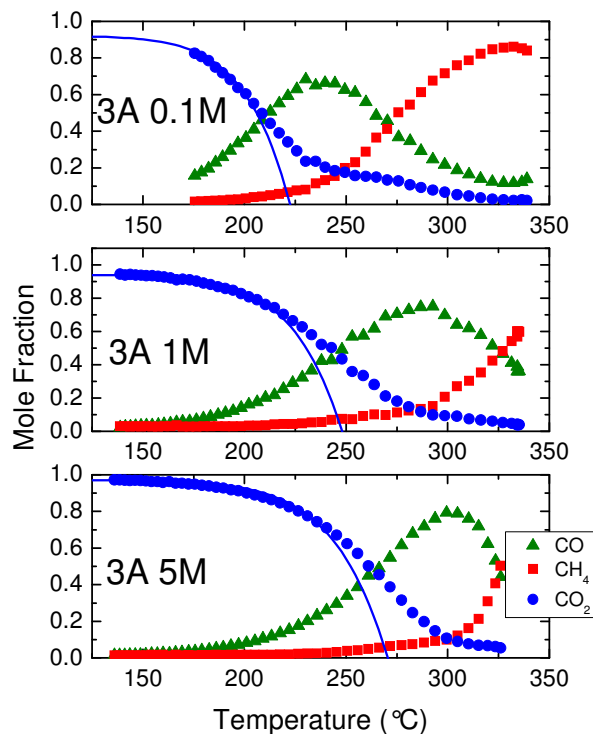


Figure 2: Temperature dependence of the exhaust gas content of Ni-zeolite 3A ion exchanged with 0.1M and 5M Ni-nitrate solutions resulting in a nickel concentration of 1, 5 and 15 at.%, respectively. The space velocity is around 1000 h^{-1} . The blue line is a fit to a simple Arrhenius type equation with equal activation energy (94 kJ/mol) for all systems for the sake of comparison using the prefactor.

The activity and selectivity of the six showcase systems vary greatly; the 5A5M system (5A zeolite exchanged with 5M Ni-nitrate solution) has highest conversion rate at nearly 100% selectivity for CH_4 . Vice versa, the reactivity of the 3A systems is slightly lower, at high selectivity for CO (compare also values in Table 1).

To be able to compare the catalytic systems, we added a fit of the CO_2 concentration to the function

$$R = 1 - k \exp\left(\frac{E_A}{RT}\right) \quad (2)$$

with a constant activation energy E_A of 94 kJ/mol as derived from the 5A5M system (which is in good agreement with the literature value of the activation energy of the methanation reaction on Ni [17]). The fits are acceptable at lower temperatures, i.e. low conversion rates, and the fit parameter k scales with the amount of irreversibly adsorbed hydrogen, i.e., the number of catalytically active sites (compare Table 1).

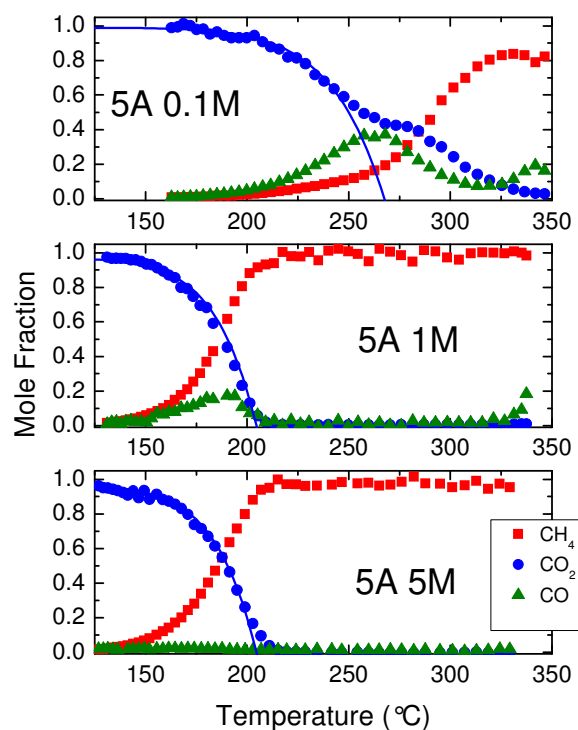


Figure 3: Temperature dependence of the exhaust gas content of Ni-zeolite 5A ion exchanged with 0.1M and 5M Ni-nitrate solutions resulting in a nickel concentration of 1.1, 2.1 and 2.5 at.%, respectively. The space velocity is around 1000 h^{-1} . The blue line is a fit to a simple Arrhenius type equation with equal activation energy (94 kJ/mol) for all systems for the sake of comparison using the prefactor.

At higher conversion rates, the formed CO may not be further reduced fast enough and therefore the catalyst produces CO. This effect is well depicted by comparing the CO_2 conversion of the 5A 5M and 5A 1M catalysts (Figure 3). These systems have a very similar Ni-content and therefore similar amount of catalytic centres. Accordingly, the CO_2 conversion is identical: what is different is the amount of CO produced at intermediate conversion rates. This difference is explained using details of the microstructure (see later).

At very low Ni-content, the CO_2 conversion drops as well as the one of the subsequent reaction steps. Still, the CO_2 conversion is relatively high leading to a high selectivity to CO (see Figure 3, catalytic activity for the 5A 0.1M system). Summarizing, the selectivity to CO is related to the relative activity of the first CO_2 hydrogenation steps (yielding CO) compared to the subsequent steps (yielding methane). In case of the 5A zeolite, this relation is influenced by the Ni-content. The 3A systems show a different behaviour: although the Ni-content varies over a much higher span than in the 5A systems (from 1 to 18% at., see Table 1), the changes of the catalytic activity and in particular of the selectivity are rather subtle (Figure 2).

The dominant product at lower temperatures is CO, further hydrogenation to methane occurs at higher temperatures only. A small difference is the temperature at which CO production peaks, the overall trend remains - in contrast to the 5 A system. This is a clear hint of the influence of the support on the catalytic activity.

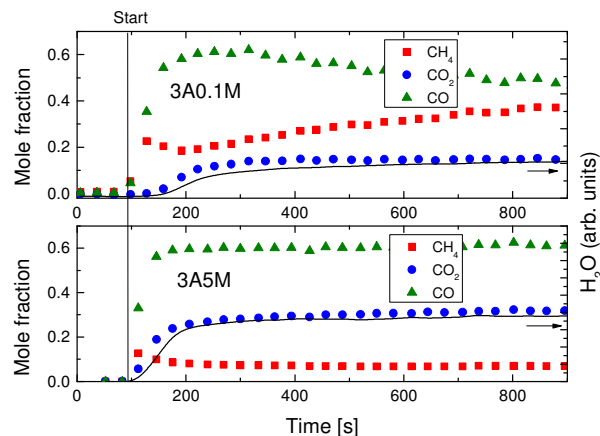


Figure 4: Isothermal measurements of the transient kinetics of a 3A0.1M (top) and 3A5M (bottom) catalyst, $T = 265^\circ\text{C}$, 20 sccm CO_2 . CO_2 was admitted at $t = 40 \text{ s}$. CO_2 , CO, and CH_4 mole fractions are shown as dots, the uncalibrated water concentrations as lines.

The above discussed catalytic activity is a temperature scan after high temperature equilibration assuming that the support, i.e., the zeolite does not adsorb any water. However, in the dry state, the zeolite has a high affinity to water, and thereby actively removes the product from the reaction centres. This so-called sorption catalysis changes the overall energy relations and turns the endothermic RWGS-reaction into an exothermic one [4] [18]. Figure 4 shows the time evolution of the gas composition at the reactor outlet at 265°C . Initially the gas contains only impurities of water and CO_2 , i.e., a conversion rate of 100%. Here, maximum amount of CO is produced. However, when the total amount of water exceeds the maximum uptake capacity, also water leaves the reactor and the reaction yield decreases. The water adsorption in the zeolite pores enhances both the formation of CO and CH_4 , in good agreement with Ref. [2] (CH_4) and Ref. [18] (CO). The relevance of each process depends also on its location, i.e., near/in the pores CH_4 cannot be formed thus enhancing CO formation, while the CH_4 formation takes place on external Ni-particles.

Structural properties of Ni zeolites

Without further investigations, the origin of the effect cannot be unambiguously assigned to the shape selectivity originating from the different pore sizes of the zeolites: the catalytic systems prepared from Ni-nitrate solutions on different supports might have different Ni-particles, i.e., overall Ni-concentration, number and size of Ni-particles, being a possible alternative origin of the effect. The difference in catalytic activity between 0.1M and 5M catalysts on the same support

(5A) supports this hypothesis. Indeed Lawson and Rase proposed that an optimum nickel crystallite size and therefore nickel distribution for highest catalytic activity exist in Ni-zeolites [19]. Furthermore, remaining Ni⁺ cationic sites in the zeolites might be catalytically active [20]. Thus, in the following we give a detailed analysis of the structural and adsorptive properties.

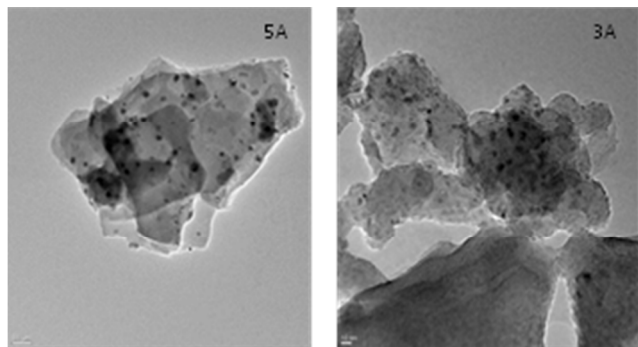


Figure 5: TEM images of Ni-particles in 5A and 3A zeolites. Ni particles are larger in 5A 5M than in 3A 0.1M. An estimation of the particle size distribution is given in **Figure 6**.

We assigned the samples by the zeolite used (“3A”, “5A”) and the concentration of the Ni-nitrate impregnation solution (“1M”) as a parameter for the overall Ni-uptake in the zeolite. This indeed corresponds approximately with the measured Ni-concentration ranging from 1 to 18 at.% for the 3A zeolite and 1 to 2.5 at.% for the 5A zeolite. Apparently, the relation is not linear: the 5A zeolite has reached its saturation level already at 2.5 at.%, the saturation level is higher for the 3A zeolite (compare also literature values for 4A zeolites: [21]). X-ray diffraction reveals only slight structural changes of the zeolites and Ni-particles with a diameter in the 2-5 nm range (Scherrer formula). Detailed insights are given by electron microscopy: SEM-pictures show regular zeolite crystals with an average size of several μm . TEM images resolve the microscopic fine structure of the Ni-particles (Figure 5): Ni particles (dark spots) are distributed across the zeolite and some areas seem to contain more particles than others. Ni particles are larger in the zeolite 5A 5M than 3A 0.1M.

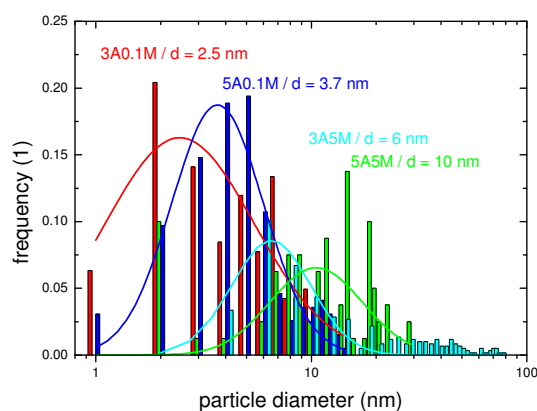


Figure 6: Size distribution of Ni-particles in 5A and 3A zeolites exchanged with 5 M and 0.1 M Ni-nitrate solutions (columns) as derived from TEM-measurements. The mean value of the size distribution is derived from fits to a log-normal statistics (lines).

The size distribution of several Ni particles from the zeolites 5A and 3A is shown in **Figure 6**. The Ni particles in zeolite 5A5M have a broad size distribution; the majority of the observable particles are ranging between 10 to 20 nm. On the contrary, Ni-particles impregnated into zeolites at low concentrations form smaller Ni-particles. However, Ni particles are larger than the nominal size of the pores of the zeolite; this means that there is a local destruction of the pores of the zeolite during the growth of the Ni particles. In addition to the majority of the particles around the indicated mean value of 6 nm, the 3A zeolite exchanged with high Ni-concentration (3A5M) has relatively large particles up to 100 nm. This is in good agreement with the maximum Ni concentration exchanged in the zeolite: while the maximum Ni-uptake in 5A zeolites is around 2.5 at.%, 3A zeolites contain up to 18 at.% Ni. However, the high Ni-concentration does not improve the catalytic activity (Table 1). This suggests that the excess concentration is due to large Ni-particles, which do not contribute significantly to the overall activity.

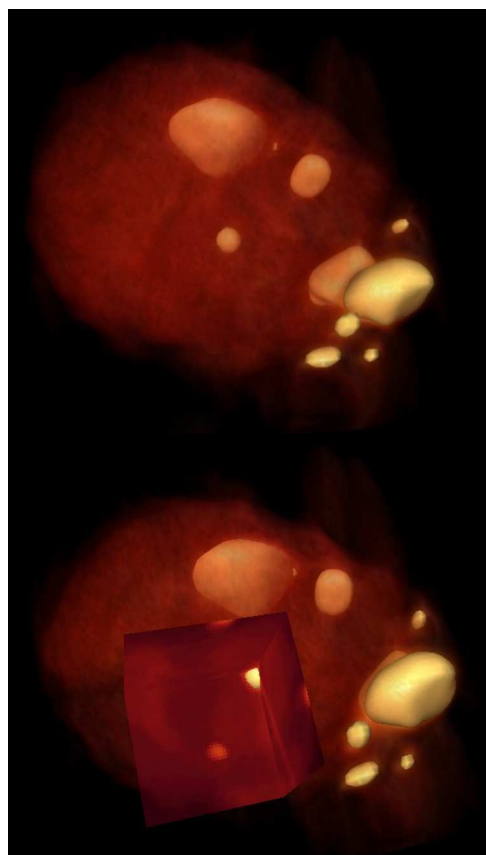


Figure 7: 3D Transmission Electron microscopy image of Ni-zeolite 5A5M. Top micrograph: Visualization of zeolite, and bottom micrograph a Ni particle inside the zeolite visualized by a corner cut. The image size is around 150 nm x 100 nm.

An important piece of information is, whether the particles are formed only on the external surface of the crystals. Electron tomography gives information on the size, shape and location of the Ni particles inside the zeolite. For this reason, STEM-tomography was conducted on the sample; the tomography clearly demonstrated that Ni-particles agglomerate not only outside the crystals, but also inside the pores (thus locally destroying the structure). **Figure 7** shows 3D reconstructed images from -90 nm crystals of 5A zeolite. The zeolite structure is shown in dark beige and the Ni particles in bright beige. To illustrate that Ni particles exist inside the zeolite crystal, a corner is cut out of the zeolite crystal. Although the TEM results provide detailed information about particle sizes larger than about 1-2 nm, it cannot be ruled out that small clusters of Ni atoms are present as well.

Ni particles also grow inside the zeolite structure of 3A zeolite as it is demonstrated in the supplementary information. The size of the Ni particles is slightly smaller in 3A zeolite (Figure 6) than in 5A zeolite. Generally speaking, the effect of the pore structure of the support on the Ni-particles is less pronounced than the effect of the Ni-concentration of the impregnation solution. Because the strong selectivity effect observed in **Figure 2** and **Figure 3** mainly depends on the choice of the support, the influence of the size of the Ni-particles is of less significance for this effect.

Shape selectivity in reactions with molecules with small kinetic diameter

Figure 8 shows hydrogen and CO₂ adsorption isotherms at room temperature for Ni exchanged 3A and 5A zeolites. The effect of the two different pore sizes of 3 Å and 5 Å, respectively, on the uptake of CO₂ (kinetic diameter, 3.3 Å) is obvious, in pure zeolites the ratio of maximum uptakes at 1 bar is around 20 (see Table 1). The same is true for CO (kinetic diameter around 3.2 Å), CH₄ (3.8 Å) and N₂ (3.6 Å). Thus, the BET surface area as extracted from the corresponding nitrogen isotherms at 78 K (Table 1) is the total surface area of 5A zeolites including internal (pore) surfaces and external (crystal) surfaces. For 3A zeolites, the surface area represents the area, which is accessible for nitrogen, i.e., the external surface, only. Smaller molecules such as water (2.65 Å) and hydrogen (2.9 Å) can be adsorbed in both pure zeolites (for hydrogen, see Table 1).

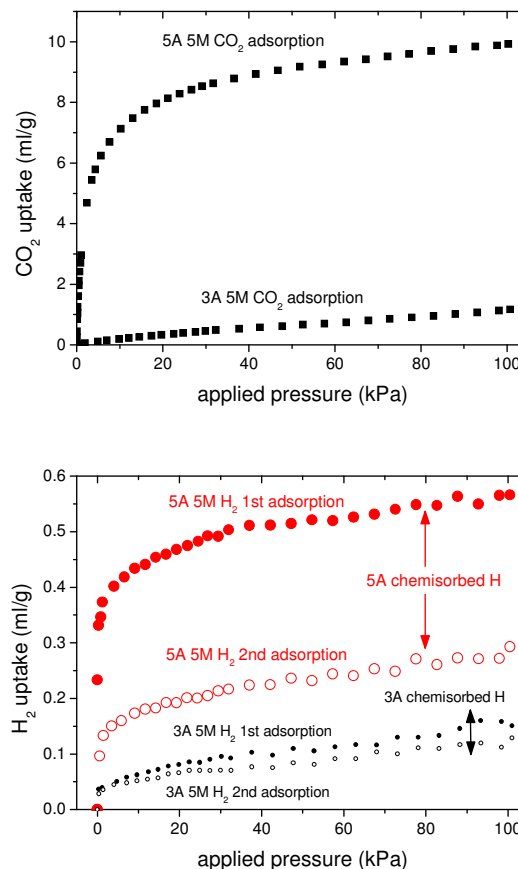


Figure 8: Hydrogen (bottom panel) and CO₂ (top) adsorption isotherms at room temperature for 3A5M and 5A5M zeolite systems. The difference between two subsequent hydrogen adsorption isotherms reflects the irreversibly adsorbed, i.e., chemisorbed hydrogen. Complete data on all investigated systems is summarized in Table 1.

Hydrogen is special, though: in Ni-impregnated zeolites, hydrogen can be chemisorbed. By performing subsequent hydrogen adsorption isotherms, the amount of chemisorbed hydrogen is determined (see Table 1, **Figure 8**).

The results of the adsorptive properties are summarized in Table 1 together with the main outcome from the catalytic testing. The interpretation is straightforward for the 5A system: The pores of the 5A zeolites are large enough to accept CO₂ and H₂, and CO as well as CH₄ can easily leave the cages. The ion exchanged systems show a similar BET-surface, and accordingly the CO₂ and H₂ uptake in physisorbed form is similar. Adding Ni corresponds to adding catalytic centres evidenced by the high fraction of irreversibly adsorbed hydrogen in the 5A5M sample.

Table 1: Basic Properties of the presented catalytic systems: Ni concentration, irreversibly and total amount of adsorbed hydrogen, BET-surface area, CO₂ uptake at 1bar CO₂ and room temperature, temperature T_{1/2} indicating 50% conversion rate, CO selectivity and pre-exponential parameter of the conversion rate *k* determined from eq. (2).

Sample	Ni-conc.	H _{chem} /H _{total}	BET	CO ₂	T _{1/2}	CO / (CH ₄ +C O ₂)	<i>k</i>
Units	at. %	ml/g	m ² /g	ml/g	(°C)	Mol/Mol	0.01 Mol/Mol
3A	0	0.02/0.29	13	2.8	-	-	-
3A0.1M	~1	0.008/0.281	17	1.23	210	1.0	0.755
3A1M	5	0.06/0.26	15	0.91	230	2.9	0.250
3A5M	18	0.03/0.13	12	1.17	260	4.0	0.105
5A	0	0.04/0.32	460	60.3	-	-	-
5A0.1M	1.1	0.009/0.265	336	55.6	260	0.6	0.12
5A1M	2.1	0.12/0.43	312	52.1	190	0.17	1.85
5A5M	2.5	0.25/0.62	330	55.0	190	0.024	1.85

The situation is different in the 3A zeolite: it accepts hydrogen molecules in the pores; the pure 3A zeolite adsorbs nearly exactly as much hydrogen as the 5A zeolite. This confirms that the inner surfaces are similar. However, these surfaces are not accessible by CO₂; maximum CO₂ uptake in 3A is a factor of 20 lower than in 5A. The BET measurements reveal only the outer surface of the 3A zeolite, which is of the same order expected from the electron microscopy measurements of the crystallite size (in the micrometre range). Increasing the Ni-content slightly enhances the amount of irreversibly adsorbed hydrogen. Simultaneously, the amount of adsorbed CO₂ and the total amount of hydrogen is reduced. Apparently, some of the pores and pore entrances of the 3A zeolite are blocked by Ni particles. This explains why despite the increase of the number of possibly active centres the total CO₂ hydrogenation rate is reduced (as evidenced by the increased temperature for 50% CO₂ conversion, see Table 1). On the other hand, the selectivity for CO is greatly enhanced.

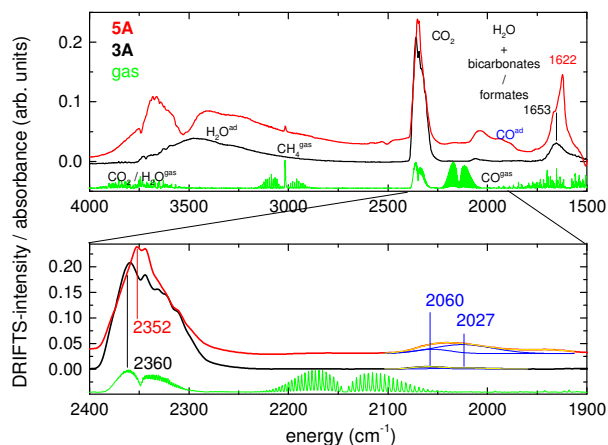


Figure 9: DRIFT spectra of Ni-loaded 3A and 5A catalysts (3A1M and 5A1M) under steady state conditions in a 8:1 H₂:CO₂ mixture at 420°C (top). The bottom graph is a magnification of the region of CO₂ and CO vibrations. The relative intensity between 3A and 5A was conserved during data handling. The gas spectrum of the product gas from a 3A catalyst is added for comparison.

The different cations of the 3A and 5A zeolites define the pore size diameters, but also the amount of Ni-ion uptake and thus eventually influence the Ni-particle size. This is the reason, why we were not able to compare samples with identical Ni particle size but different pore sizes. Some of the observed effect might thus originate from different catalytic properties of the corresponding Ni-particles. Although we have presented several indirect evidences of the dominant influence of the shape selectivity on the selectivity, a final proof is missing. To do so, we employed diffuse reflectance Fourier transform infrared spectroscopy (DRIFTS) combined with mass spectrometry. By utilizing this technique it is possible to identify active adsorbates and follow the surface site occupancy during reaction. After equilibration of the catalyst in an Ar/H₂ mixture at the desired temperature a DRIFT spectrum was taken prior to introduction of the reactants. The first spectrum is taken as reference of the clean catalyst surface and is subtracted from all following spectra hence only showing changes due to changes of adsorbates on the surface of the catalyst. The thus measured DRIFT spectra of Ni on zeolite 3A and 5A after long-term exposure to a H₂/CO₂/Ar-mixture at 420°C (“steady state”) are shown in **Figure 9**. For comparison, a gas infrared spectrum of the product gas from a 3A catalyst is added. Assignment and interpretation of the spectra is straightforward: mainly CO₂, water, and CO are adsorbed on the zeolite and on the Ni-particles. Formates (1653 cm⁻¹) and bicarbonates (1622 cm⁻¹) coordinated to the zeolite are observed especially on 5A zeolite. The signals of CO are shifted by ~100 cm⁻¹ compared to those in the gas spectrum, indicating strong CO-Ni interaction resulting in the formation of subcarbonyl (2067 cm⁻¹) and linear carbonyl (2030 cm⁻¹) species chemisorbed to Ni. [22] The small differences in energy between 3A and 5A zeolites (originating from a different distribution of subcarbonyl and linear carbonyl groups, see inset in **Figure 9** [23]) and in intensity as measured under identical conditions

are attributed to a lower coverage of CO on Ni in 3A zeolite. The adsorption strength of CO on Ni is thus similar suggesting a similar catalytic behaviour of the Ni-particles in 3A and 5A zeolites. An important difference in the spectra is related to the CO₂ stretching vibrations that are stronger and slightly shifted in 5A zeolite compared to the 3A zeolite, which exhibits similar features to the gas spectrum. This reflects significant interaction of CO₂ with the pores of the 5A zeolite (despite the high temperature) [24], and negligible adsorption in 3A zeolite. This is in perfect agreement with the measurement of the isotherms (Figure 8), and the idea of the shape selectivity. CO₂ adsorption takes place on/in the zeolite support - Ni-particles inside the 5A zeolite can thus be reached by CO₂, while the ones inside 3A zeolite are attainable only to a lesser extent. This observation partly explains the selectivity towards CO (CH₄ produced inside the pores cannot leave the crystal) observed in the latter type of zeolite.

The Sabatier reaction is a complex surface reaction transferring eight hydrogens and electrons to one carbon starting from the reduction of CO₂ to COOH and CO. Calculations for the electro-catalytic reduction of CO₂ on Pt suggest that subsequently CO is fully reduced and four hydrogens are added giving methane [25]. Different pathways are possible, though: additional hydrogen may be added to CO before oxygen is removed as water. However, then a possible by-product is methanol, which was not observed. Furthermore, production of CO is suppressed, when water is removed from the reaction by adsorption in the zeolite support. This indicates that CO is reduced by the formation of water – in line with the pathway described above. The first steps of the CO₂ hydrogenation reaction are similar on all discussed systems: the fit to the temperature dependence of CO₂ conversion is satisfying for all systems; main differences appear during the subsequent steps. The ratio between first and subsequent hydrogenation steps defines the selectivity to methane or CO: if the later steps converting CO into methane are fast, CO is an impurity only; if these steps are rate-limiting, the selectivity for CO is high. With the assumption that the Ni-particles are comparable (Figure 6), the reaction steps from CO to methane must be linked to the (internal) surface of the corresponding zeolite to explain the different selectivity. Ni-ions or atoms inside the pores of the zeolites are renowned for their catalytic activity [20]. These sites alone cannot be responsible, because predominate methane yield is not found for small overall Ni-concentration (Figure 2), but for systems containing bigger Ni-particles. However, the combination of processes on the zeolite surface and the Ni-particles (e.g., at the metal – oxide interface) seems to guarantee a full reduction of CO₂ to methane in the 5A system. In the 3A system, this interaction is only possible at the external crystal surfaces, thus here the reduction to CO is fast and further reduction to methane is relatively slow. Strong hint for this is found by DRIFTS by the occurrence of strong peaks in the 5A system, which are attributed to intermediates of the reaction (carbonates, formates, see Figure 9). The 3A spectra are very similar but these peaks weaker, indicating that not the

chemistry of the zeolite surface differs strongly between 3A and 5A (e.g., the acidity), but its accessibility, i.e. the pore size. Investigations on the dynamics of these surface species giving further evidence on this hypothesis will be presented elsewhere.

At higher temperatures, the conversion of CO to CH₄ is increased relative to the production of CO and thereby the selectivity drops again. The effect of the shape selectivity may be enhanced, if a zeolite support can be developed exactly matching the proper molecule diameters to allow the adsorption of CO₂ in the pores but hindering the formation of CH₄, i.e., a pore size d of $3.8 \text{ \AA} > d > 3.3 \text{ \AA}$. This idea is corroborated by comparing the activities of the two 3A samples: although the Ni-concentration scales with the active sites, while the BET-surface and CO₂ uptake and with them the catalytic activities (i.e. k) do not. The amount of CO₂-uptake and thus the accessibility to the pores (shape selectivity) seems to be of higher relevance than the number of hydrogen dissociation sites.

100% selectivity towards CO is never possible with this setup because of thermodynamics. An observed CO/(CH₄+CO₂) ratio of 4 (Table 1) is near to the thermodynamically possible value, at which ΔG is still negative at the corresponding temperature and conversion [18], [26]. Utilizing the so-called sorption effect [18], in which the reaction enthalpy of the RWGS reaction is decreased towards negative values by the exothermic adsorption of water in zeolites, a higher selectivity is possible. First experiments indeed show the desired enhancement of the CO-selectivity for the 3A samples. However, additional difficulties associated with coking and blocking of the small pores occur, and will be published elsewhere [27].

Conclusions

In this paper, we demonstrate the extreme sensitivity of the reaction kinetics of CO₂ hydrogenation on the nanostructure of sorption catalysts. The Sabatier reaction catalysed by Ni-particles on zeolite support is greatly enhanced, if the pore size of the support is larger than 5A, pore sizes of 3A reduce the overall conversion rate and the selectivity for methane. Thus, Ni on 3A zeolites may be used as low temperature catalysts for the reversed water-gas shift reaction. The kinetic effect is improved, if the water adsorption capability of the zeolite is used: here, the endothermic reaction is turned into an exothermic one using the heat of adsorption in the zeolite. The experiments also reveal a dependence of the reaction yield on the CO₂ uptake capability, which is linked to that of the CH₄ uptake (similar kinetic diameter). Thus, the overall catalytic activity producing selectively CO is relatively low. This indicates the relevance of concept of “shape selectivity of nanoporous composite catalysts” also for small molecules, i.e., for the production of renewable energy carriers (CO, CH₄). Future prospect may be the preparation of porous hosts with appropriate pore size d of $3.8 \text{ \AA} > d > 3.3 \text{ \AA}$. The design of such

zeolites has recently been demonstrated [28], [29]. In addition, it is shown that the enhancement of the reaction yield by water adsorption in the zeolite pores is only effective if adsorption and catalytic reaction take place in the near vicinity. The sorption enhancement may therefore be described as a “reversed spillover effect” (compare, e.g., Ref. [30]). Though requiring new reactor concepts, the sorption enhancement for methane has been demonstrating to increase the energy efficiency of the methanation significantly [5]. With improving the nano-structured sorption support, an equally high improvement might be possible for the reversed water-gas shift as well.

Acknowledgements

This work was financially supported by the Swiss National Science Foundation (grant agreement 407040_153928) the European Commission, Grant agreement No. FP7–284522 (infrastructure program H2FC).

Notes and references

^aLaboratory Advanced Analytical Technologies, ^bLaboratory for Hydrogen & Energy, and ^cElectron Microscopy Center, Empa, Swiss Federal Laboratories for Materials Science and Technology, Überlandstrasse 129, CH-8600 Dübendorf, Switzerland;

^dChemical Engineering, Delft University of Technology, Julianalaan 136, 2628 BL Delft, The Netherlands;

^eLaboratory of Materials for Renewable Energy (LMER) Basic Science Faculty Institute of Chemical Sciences and Engineering (ISIC) École polytechnique fédérale de Lausanne (EPFL) PH A2 354, Station 3 CH-1015 Lausanne, Switzerland

^fPaul Scherrer Institute, OLG/411, 5232 Villigen – PSI, Switzerland

References

- [1] A. Brunetti, E. Drioli and G. Barbieri, “Energy and mass intensities in hydrogen upgrading by a membrane reactor,” *Fuel Processing Technology*, vol. 118, p. 278, 2014.
- [2] A. Borgschulte, N. Gallandat, B. Probst, R. Suter, E. Callini, D. Ferri, Y. Arroyo, R. Erni, H. Geerlings and A. Züttel, “Sorption enhanced CO₂ methanation,” *Phys. Chem. Chem. Phys.*, vol. 15, p. 9620, 2013.
- [3] D. J. Darensbourg, C. G. Bauch and C. C. Ovalles, “Mechanistic aspects of catalytic carbon dioxide methanation,” *Rev. Inorg. Chem.*, vol. 7, pp. 315-339, 1985.
- [4] W. Haije and H. Geerlings, “Efficient Production of Solar Fuel Using Existing Large Scale,” *Environ. Sci. Technol.* 45, p. 8609–8610, 2011.
- [5] S. Walspurger, G. D. Elzinga, J. W. Dijkstra, M. Saric and W. Hajie, “Sorption enhanced methanation for substitute natural gas production: Experimental results and thermodynamic considerations,” *Chemical Engineering Journal*, vol. 242, pp. 379-386, 2014.
- [6] J. Norskov, T. Bligaard, J. Rossmeisl and C. H. Christensen, “Towards the computational design of solid catalysts,” *Nature Chemistry*, vol. 1, p. 37, 2009.
- [7] T. Degnan, “The implications of the fundamentals of shape selectivity for the development of catalysts for the petroleum and petrochemical industries,” *J. Catal.*, vol. 216, pp. 32-46, 2003.
- [8] B. Smit and L. Maesen, “Towards a molecular understanding of shape selectivity,” *Nature*, vol. 451, p. 671, 2008.
- [9] S. T. Sie, “Past, present and future role of microporous catalysts in the petroleum industry,” *Studies in Surface Science and Catalysis*, vol. 85, pp. 587-631, 1994.
- [10] R. Gounder and E. Iglesia, “The catalytic diversity of zeolites: confinement and solvation effects within voids of molecular dimensions,” *Chem. Commun.*, vol. 49, p. 3491, 2013.
- [11] J. Bao and N. Tsubaki, “Core-shell catalysts and bimodal catalysts for Fischer-Tropsch synthesis,” *Catalysis*, vol. 25, pp. 216-245, 2012.
- [12] M. D. Lechner, D'Ans Lax Taschenbuch für Chemiker und Physiker Bd. 1, Berlin Heidelberg New York: Springer, 1992.
- [13] E. Roland and P. Kleinschmidt, “Zeolites,” in *Ullmann's Encyclopedia of industrial chemistry*, Heidelberg, Wiley VCH, 2012, p. 687.
- [14] H. Gesser, A. Rochon, A. Lemire, K. Masters and M. Raudsepp, “Pressure dependence of methane encapsulation in type 3A zeolites,” *Zeolites*, vol. 4, no. 1, pp. 22-24, 1984.
- [15] J. Gao, C. Jia, M. Zhang, F. Gu, G. Xu and F. Su, “Effect of nickel nanoparticle size in Ni-Al₂O₃ on CO methanation reaction for the production of synthetic natural gas,” *Catal. Sci. Technol.*, vol. 3, p. 2009, 2013.
- [16] R. van Harveld and F. Hartog, “Influence of Metal Particle Size in Nickel-on-Aerosil Catalysts on Surface Site Distribution, Catalytic Activity, and Selectivity,” *Advances in Catalysis*, vol. 22, p. 75, 1972.
- [17] T. van Herwijnen, H. van Doesburg and W. A. de Jong, “Kinetics of the Methanation of CO and CO₂ on a Nickel Catalyst,” *J. Catal.*, vol. 28, pp. 391-402, (1973).
- [18] B. T. Carvill, J. R. Hufton, M. Anand and S. Sircar, “Sorption-Enhanced Reaction Process,” *AIChEJ*, vol. 42, pp. 2765-2772, 1996.
- [19] J. D. Lawson and H. F. Rase, “Ni-zeolites,” *Ind. Eng. Chem. Prod. Res. Develop.*, vol. 9, p. 317, 1970.
- [20] A. I. Serykh and M. D. Amiridis, “Formation and Thermal Stability of Ni⁺ Cationic Sites in Ni-ZSM-5,” *J. Phys. Chem. C*, vol. 111, p. 17020, 2007.
- [21] I. J. Gal, O. Janković, S. Malčić, P. Radovanov and T. M., “Ion-exchange equilibria of synthetic 4A zeolite with Ni²⁺, Co²⁺, Cd²⁺ and Zn²⁺ ions,” *Trans. Faraday Soc.*, vol. 1008, p. 999, 1971.
- [22] L. Surnev, Z. Xu and J. J. Yates, “IRAS Study of the adsorption of CO on Ni(111) – interrelation between various bonding modes of chemisorbed CO,” *Surf. Sci.*, vol. 201, pp. 1-13, 1988.

- [23] G. Martra, H. M. Swaan, C. Mirodatos, M. Kermarec and C. Louis, "Sintering of Ni/SiO₂ Catalysts Prepared by Impregnation and Deposition-Precipitation During CO Hydrogenation," in *Catalyst Deactivation*, Amsterdam, Elsevier Science, 1997, p. 617.
- [24] V. B. Kazansky, V. Y. Borovkov, A. I. Serykh and M. Bulow, "First observation of the broad-range DRIFT spectra of carbon dioxide adsorbed on NaX zeolite," *Phys. Chem. Chem. Phys.*, vol. 1, pp. 3701-3702, 1999.
- [25] C. Shi, C. P. O'Grady, A. A. Peterson, H. A. Hansen and J. K. Norskov, "Modeling CO₂ reduction on Pt(111)," *Phys. Chem. Chem. Phys.*, 2013.
- [26] J. Gao, Y. i Wang, Y. Ping, D. Hu, G. Xu, F. Gu and F. Su, "A thermodynamic analysis of methanation reactions of carbon oxides for the production of synthetic natural gas," *RSC Advances*, vol. 2, p. 2358-2368, 2012.
- [27] A. Borgschulte, *to be published*, 2015.
- [28] X. Gu, Z. Tang and J. Dong, "On-stream modification of MFI zeolite membranes for enhancing hydrogen separation at high temperature," *Microporous and Mesoporous Materials*, vol. 111, p. 441, 2008.
- [29] Z. Tang and J. Dong, "Internal surface modification of MFI-type zeolite membranes for high selectivity and high flux for hydrogen," *Langmuir*, vol. 25, p. 4848, 2009.
- [30] W. C. Conner and J. L. Falconer, "Spillover in heterogenous catalysis," *Chem. Rev.*, vol. 95, p. 759, 1995.
- [31] T. Montanari, I. Salla and G. Busca, "Adsorption of CO on LTA zeolite adsorbents: An IR investigation," *Microporous and Mesoporous Materials*, vol. 109, pp. 216-222, 2008.
- [32] E. Derouane and Z. Z. Gabelica, "A Novel Effect of Shape Selectivity: Molecular Traffic Control in ZSM-5," *J. Catal.*, vol. 65, p. 486, 1980.
- [33] A. I. Serykh and M. D. Amiridis, "Formation and Thermal Stability of Ni⁺ Cationic Sites in Ni-ZSM-5," *J. Phys. Chem. C*, vol. 111, pp. 17020-17024, 2007.